Third-harmonic generation microscopy of undeveloped photopolymerized structures

Leevi Kallioniemi,[1,2] **Shambhavee Annurakshita,**[1,2] **and Godofredo Bautista**[1,*]

[1]*Photonics Laboratory, Tampere University, Korkeakoulunkatu 3, 33720, Tampere, Finland*
[2]*These authors contributed equally.*
[*]*godofredo.bautista@tuni.fi*

Abstract: Third-harmonic generation (THG) microscopy is demonstrated as a powerful technique to visualize undeveloped photopolymerized microstructures within a negative photoresist film. By comparing the THG microscopy images of developed and undeveloped single-photon polymerized structures in a SU-8 film, THG was found to provide sufficient contrast for distinguishing polymerized and unpolymerized regions. This also suggests that the technique can be used as a complementary technique to visualize the effect of photoresist development where microstructure shrinkage could occur. In addition, we applied the technique to visualize a three-photon polymerized microstructure that was fabricated in the same microscopy setup. This demonstrates the potential of the technique for *in situ* microscopy of photopolymerized microstructures in three dimensions.

1. Introduction

Photopolymerization is the process of creating polymers by light absorption. Photopolymerization also provides a way to produce submicron-sized features that are highly localized within the three-dimensional focal volume by altering the chemical properties of a photosensitive polymer through multiphoton absorption [1–3]. It is a widely used technique for fabricating a variety of microscopic elements that have been valuable in many fields [4–6]. To date, the visualization of photopolymerized structures remains a major challenge. To evaluate the quality of the photopolymerized structures, characterization is usually performed right after the photoresist is developed. For example, scanning electron microscopy (SEM) is employed. However, due to sample preparation effects in SEM, the technique generally prohibits sample reuse. Furthermore, the technique is mainly surface-sensitive so it cannot be used to examine embedded structures. The chemical sensitivity of X-ray microscopy could be also used to visualize developed photoresists [7]. The technique, however, is not easily available since it requires access to a synchrotron radiation facility. Excluding optical sectioning and high spatial resolution effects, photoresists have been also visualized using dark-field microscopy [8], infrared microscopy [9] and optical coherence tomography [10].

The *in situ* evaluation of photopolymerization remains desired allowing one to directly visualize the structures before sample processing and if possible, perform adjustments during the exposure. Although bright-field illumination can be coupled easily to an existing single or multiphoton photopolymerization setup, the technique provides only a general overview of the photopolymerized region concealing submicron-sized details that are highly localized in three dimensions. By using photoresists that have been incorporated with external agents such as fluorophores, the photopolymerized structures could be visualized at high contrast [11,12]. However, the technique relies heavily on the compatibility of the photoresist and external agents used. On the other hand, label-free characterization of the photopolymerized structures has been demonstrated *in situ* with chemically-sensitive coherent anti-Stokes Raman microscopy, a four-wave mixing process [13]. However, the technique requires the use of two laser lines that

are used to drive the CARS signal and another laser line for photopolymerization. Recently, two-photon luminescence was used to examine unlabeled and undeveloped photopolymerized microstructures [14]. The polymerization and imaging techniques use the same excitation laser allowing direct integration to an existing two-photon polymerization setup, where the microscopy part can be performed directly after exposure. Although the technique is label-free, the technique generally requires photoinitiators that exhibit photoluminescence quenching. Third-harmonic generation (THG) microscopy, which relies on the changes of the effective third-order nonlinear-optical susceptibility of materials placed in the focal volume of the microscope [15,16], has been also useful in visualizing unlabeled and developed photopolymerized microstructures [17,18]. To date, the demonstration of THG to monitor the photopolymerization and visualize undeveloped photopolymerized structures is still unexplored. Thus, the development of complementary microscopy techniques to visualize photopolymerized microstructures *in situ*, in three dimensions and at high resolution is important.

In this paper, we present the capability of THG microscopy to visualize undeveloped photopolymerized structures. By comparing the THG microscopy images of developed and undeveloped single-photon polymerized structures in a SU-8 film, we found that THG provides sufficient contrast to distinguish polymerized and unpolymerized regions in a polymer bath. This implies that the technique can be used to visualize the effect of sample processing such as photoresist development. In addition, we applied the technique to visualize a three-photon polymerized microstructure that was fabricated in the same microscopy setup. This demonstrates the potential of the technique for *in situ* imaging of photopolymerized microstructures in three dimensions.

2. Materials and methods

The schematic of the optical setup used in our experiments is shown in Fig. 1. Previously, our NLO microscopy setup has been used to characterize a wide variety of different nanostructures [19–21]. Our microscope utilizes a femtosecond laser (wavelength of 1060 nm, repetition rate of 80 MHz, pulse length of 140 fs,) as an excitation source. The laser beam is spatial-filtered, expanded, and directed into a high numerical aperture (NA) microscope objective (Nikon CFI LU Plan Fluor Epi P, NA of 0.8, infinity corrected, 50× magnification). The beam is focused into the sample, which is mounted on a computer-controlled three-dimensional piezo-scanning system. The scanning system has a maximum scanning range of 75 μm × 75 μm × 50 μm along the x, y, and z directions. The back-scattered signal is collected by the same objective, and the THG signal is separated from the fundamental beam using appropriate filters (e.g., Semrock, BSP01-785R-25 and FF01-356/30-25). The THG signal is directed onto a cooled photomultiplier tube. To acquire a raster scanning image, the sample is moved in relation to the beam. For each relative location of the sample and the beam, THG signal is collected and plotted using a custom-designed LabVIEW program. Power is controlled using an attenuator. Polarization was controlled using a half-wave plate. THG imaging was done using a linearly polarized beam at 5 mW, which was low enough not to cause any unwanted effects. The pixel dwell time is 50 ms and image resolution is 100 pixels × 100 pixels. To induce three-photon polymerization in the photoresist, we used the same excitation arm of the THG microscope with input power of 20 mW. During photopolymerization, the PMT was not operated and the piezo stage-scanner was programmed to follow a contour with writing speed of 6 μm/s. After photopolymerization, the input power was decreased back to 5 mW and the region containing the photopolymerized grid structure was imaged using THG.

SU-8 photoresist was chosen because it is a popular photoresist [22]. Two photoresist film samples were prepared by spin coating a droplet of 1 ml of negative photoresist of SU-8 5 on top of the silicon wafer at spin speed of 5000 rpm and acceleration of 250 rpm in 1 minute. The films were then prebaked at 65°C for 1 min and then at 95°C for 3 min. The films were then allowed to cool down to the temperature 40°C. The films were made in contact with a photomask (e.g.,
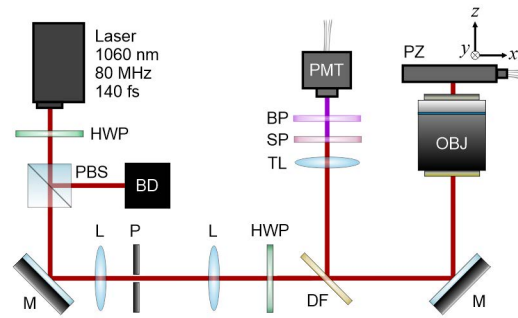
Fig. 1. Schematic diagram of THG microscopy setup. The microscope is powered by a laser source (1060 nm, 80 MHz, 140 fs,) and composed of the following components: half-wave plate (HWP), polarizing beamsplitter (PBS), beam dump (BD), lenses (L), mirrors (M), pinhole (P), dichroic filter (DF), microscope objective (OBJ), piezo-scanners (PZ), tube lens (TL), shortpass filter (SP), bandpass filter (BP) and photomultiplier tube (PMT).

square arrays with side length of 20 µm and periodicity of 4 µm) and exposed at the wavelength of 365 nm for 16 seconds in an optical lithography system (EVG 620). The exposed films were then post baked at 65°C for 1 min and then at 95°C for 3 min. One of the samples was developed by rinsing it in the developer (MR Dev) for 1-2 min and then rinsed with the isopropanol and deionized water. The resulting samples were imaged in a bright-field microscope (Nikon Eclipse LV150NA) using green filter to avoid extra exposure during optical imaging. To confirm the physical dimensions of the photopolymerized structure in the developed film, a scanning electron microscope (Zeiss ULTRA-55) was used. For the *in situ* three-photon polymerization experiment, a 10-µm thick SU-8 5 film on top of silicon wafer was prepared separately.

3. Results and discussion

As shown in Fig. 2(a), the developed sample exhibits outlines that mark the locations of the photopolymerized square structures. The structures also seem to appear uniform. However, without prior knowledge about the photomask design and photoresist, it is hard to pinpoint the polymerized and unexposed unpolymerized regions. The contrast between the polymerized and unpolymerized regions is even lower in the undeveloped sample (Fig. 2(b)). Note also that in Fig. 2(b), the brightfield image also suggests that the film thickness is uniform. As shown in Figs. 2(c) and 2(d), square structures were indeed formed in the developed sample. Close inspection of the structure (Fig. 2(d)) revealed that the top edges are not uniform and the structures are a bit tapered. These submicron-sized features cannot be detected in the bright-field microscopy images.

We first present the THG microscopy results of the photopolymerized structures in the developed sample. As shown in Fig. 3(a), the square structures clearly stand out from the background. This result implies that THG can be used to identify photopolymerized microstructures at high contrast and consistent with earlier findings [17,18]. Here, the background THG signal is about 10% of the THG signals from the square structure. We then focused on imaging a single square structure. As shown in Fig. 3(b), the THG image of the square is not uniform. Since THG is very sensitive to inhomogeneities at the focus, it is possible that the varied THG intensities reflect the nonuniform distribution of formed polymers throughout the volume of the square structure. Furthermore, there is a significant variation of THG signals near the edges of the structure. This is further corroborated by the corresponding THG scan along the longitudinal direction of the square structure (Fig. 3(c)), which revealed variations of the THG signals near the edge. These results indicate that the edges are nonuniform and agree with the SEM finding (Fig. 2(d)).
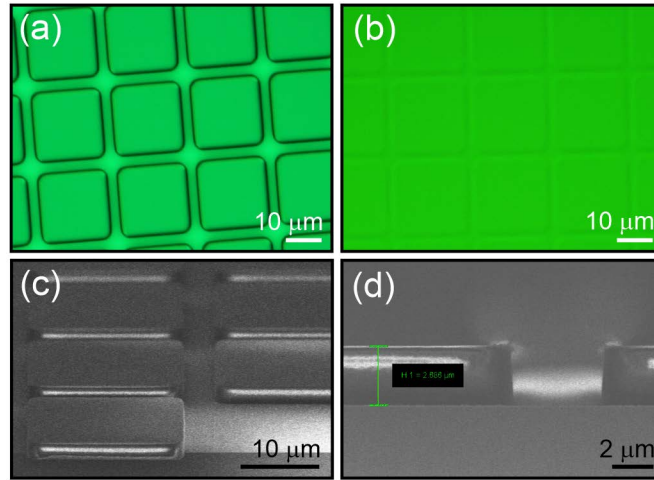
Fig. 2. Bright-field optical microscopy images of the (a) developed and (b) undeveloped photopolymerized structures in a SU-8 film on silicon wafer. (c) Oblique and (d) side-view SEM pictures of the developed film.
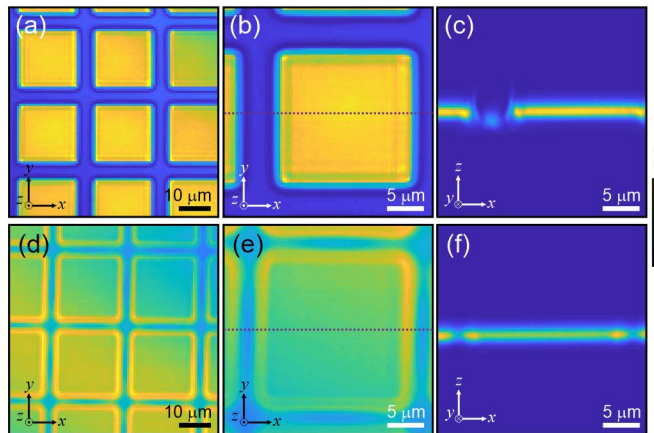

Fig. 3. Transversal *xy* THG microscopy images of the (a,b) developed and (d,e) undeveloped photopolymerized structures in a SU-8 film on silicon wafer. Longitudinal *xz* THG microscopy images of the (c) developed and (f) undeveloped samples. The locations of the longitudinal planes are marked in (b,e). Image resolution is 100 pixels × 100 pixels.

Next, we present the THG microscopy results of the undeveloped structures. As shown in Fig. 3(d), the photopolymerized structures give higher THG signals than the background. There is also a significant variation in the THG signals of the individual squares, which suggests the nonuniform distribution of polymers. Also, the film thickness in this region might not be uniform in contrast to the earlier suggestion of the representative brightfield image. This further exemplifies the extreme sensitivity of THG to the quality of interfaces, with unique features that usually remain undetectable in classic imaging techniques like brightfield and differential interference contrast techniques. The THG image of the individual square structure also revealed that the features near the edges are nonuniform (Fig. 3(e). Such variations are also reflected in the corresponding THG image along the longitudinal direction (Fig. 3(f)).

There are clear differences in the THG images of the developed and undeveloped structures. First, even if the samples were prepared identically prior to sample development, the spatial extent of the photopolymerized structures that were examined by THG are not the same. For example, the developed square structures were found to be smaller than their undeveloped counterparts, which might have been influenced by sample development. This is because acrylate-based resins and negative-tone photoresists typically exhibit shrinkage and distortions during the exposure and development stages [23,24]. Second, the image contrast of the THG images of undeveloped sample was found to be lower than the ones from the developed sample. This is due to the fact the in the developed sample, the presence of air drastically changes the effective third-order nonlinear-optical susceptibility at the focal volume. In the THG images of the undeveloped sample, the background signal is about half of the THG signals from the photopolymerized region. However, this is still better than what is achieved under a bright-field microscope.

To demonstrate the capability of THG microscopy to examine the details of developed and undeveloped square structures, high-resolution scans were performed. As seen in Figs. 4(a) and 4(b), the corners and edges of the structures are not smooth as exemplified by the variations in the THG signals. Even at moderate image contrast, THG microscopy was able to reveal that the edges of the photopolymerized square structure in the undeveloped sample are not uniform (Fig. 4(c)). It is also worth noting that due to the intrinsic optical sectioning capability of THG microscopy, three-dimensional imaging of submicron-sized features in the vicinity of the photopolymerized microstructures is feasible. This provides a nondestructive way to examine the quality of the undeveloped microstructures.

Our results imply that THG microscopy can be used as an *in situ* diagnostic tool to visualize photopolymerized microstructures even before development. For example, this approach could be integrated directly in a three-photon polymerization setup. To prove this point, we performed three-photon polymerization [3] experiments on a thick SU-8 film on silicon wafer using the same laser and microscopy setup. Here, the piezo-scanners were pre-programmed to move serially following a target structure, e.g., 4×4 grid pattern. Upon laser irradiation, three-photon polymerization is induced only at the pre-programmed locations. After exposure, we subsequently performed THG imaging of the area containing the polymerized region at the same focal plane. Shown in Fig. 4(d) is the THG microscopy image of a three-photon polymerized grid structure in a polymer bath. Even if the contrast in the THG image is not high, the polymerized regions are still seen against the background. Imaging this structure especially those voxels that were produced near the photopolymerization threshold could be very difficult to see with bright-field microscopy. We also disregard the possibility that the grid structure was created due to two-photon polymerization because SU-8 is highly transparent at 530 nm, which is the two-photon polymerization wavelength of our excitation laser. However, since the same laser was used in three-photon photopolymerization and THG microscopy, the input power used in THG should be low and chosen well so it avoids further polymerization. This balance should be set particularly when studying photoresists of specific absorption properties.
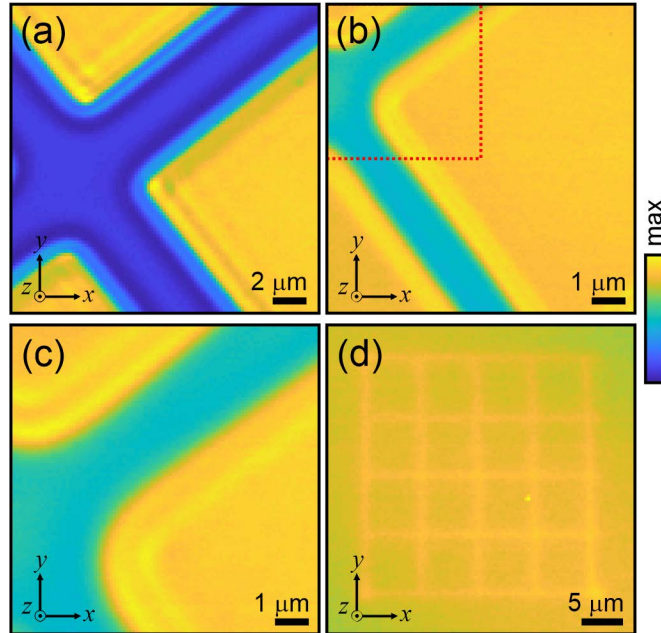
Fig. 4. High-resolution transversal *xy* THG microscopy images of the (a) developed and (b,c) undeveloped photopolymerized structures in a SU-8 film on silicon wafer. The THG image in (c) is marked in (b). (d) Transversal *xy* THG microscopy image of a three-photon polymerized microstructure in a thick SU-8 film on silicon wafer. Image resolution is 100 pixels × 100 pixels.

4. Summary

In summary, the capability of THG microscopy to visualize undeveloped photopolymerized structures was demonstrated. THG was found to provide sufficient contrast in distinguishing polymerized and unpolymerized regions in a polymer bath. The technique could be used to visualize the effect of photoresist development (e.g., shrinkage). The technique was also used to visualize a three-photon polymerized microstructure that was fabricated in the same microscopy setup, demonstrating its potential for *in situ* imaging of photopolymerized microstructures in three dimensions.

Disclosures

The authors declare no conflicts of interest.

References

1. C. N. LaFratta, J. T. Fourkas, T. Baldacchini, and R. A. Farrer, "Multiphoton fabrication," Angew. Chem., Int. Ed. **46**(33), 6238–6258 (2007).
2. S. Kawata, H. B. Sun, T. Tanaka, and K. Takada, "Finer features for functional microdevices," Nature **412**(6848), 697–698 (2001).
3. M. Farsari, G. Filippidis, and C. Fotakis, "Fabrication of three-dimensional structures by three-photon polymerization," Opt. Lett. **30**(23), 3180–3182 (2005).
4. J. Serbin, A. Egbert, A. Ostendorf, B. N. Chichkov, R. Houbertz, G. Domann, J. Schulz, C. Cronauer, L. Fröhlich, and M. Popall, "Femtosecond laser-induced two-photon polymerization of inorganic–organic hybrid materials for applications in photonics," Opt. Lett. **28**(5), 301–303 (2003).
5. P. Tayalia, C. R. Mendonca, T. Baldacchini, D. J. Mooney, and E. Mazur, "3D cell-migration studies using two-photon engineered polymer scaffolds," Adv. Mater. **20**(23), 4494–4498 (2008).
6. H. B. Sun, S. Matsuo, and H. Misawa, "Three-dimensional photonic crystal structures achieved with two-photon-absorption photopolymerization of resin," Appl. Phys. Lett. **74**(6), 786–788 (1999).
7. L. Muntean, R. Planques, A. L. D. Kilcoyne, S. R. Leone, M. K. Gilles, and W. D. Hinsberg, "Chemical mapping of polymer photoresists by scanning transmission x-ray microscopy," J. Vac. Sci. Technol., B: Microelectron. Nanometer Struct. **23**(4), 1630 (2005).
8. S. Kimura and T. Wilson, "Confocal scanning dark-field polarization microscopy," Appl. Opt. **33**(7), 1274–1278 (1994).
9. B. Dragnea, J. Preusser, J. M. Szarko, S. R. Leone, and W. D. Hinsberg, "Pattern characterization of deep-ultraviolet photoresists by near-field infrared microscopy," J. Vac. Sci. Technol., B: Microelectron. Nanometer Struct. **19**(1), 142–152 (2001).
10. J. Choi, K. S. Lee, J. P. Rolland, T. Anderson, and M. C. Richardson, "Nondestructive 3-D imaging of femtosecond laser written volumetric structures using optical coherence microscopy," Appl. Phys. A: Mater. Sci. Process. **104**(1), 289–294 (2011).
11. B. H. Cumpston, S. P. Ananthavel, S. Barlow, D. L. Dyer, J. E. Ehrlich, L. L. Erskine, A. A. Heikal, S. M. Kuebler, I. Y. S. Lee, D. McCord-Maughon, J. Qin, H. Röckel, M. Rumi, X. L. Wu, S. R. Marder, and J. W. Perry, "Two-photon polymerization initiators for three-dimensional optical data storage and microfabrication," Nature **398**(6722), 51–54 (1999).
12. H. B. Sun, T. Tanaka, K. Takada, and S. Kawata, "Two-photon photopolymerization and diagnosis of three-dimensional microstructures containing fluorescent dyes," Appl. Phys. Lett. **79**(10), 1411–1413 (2001).
13. T. Baldacchini and R. Zadoyan, "*In situ* and real time monitoring of two-photon polymerization using broadband coherent anti-Stokes Raman scattering microscopy," Opt. Express **18**(18), 19219–19231 (2010).
14. E. Yulianto, S. Chatterjee, V. Purlys, and V. Mizeikis, "Imaging of latent three-dimensional exposure patterns created by direct laser writing in photoresists," Appl. Surf. Sci. **479**, 822–827 (2019).
15. J. Squier, M. Müller, G. Brakenhoff, and K. R. Wilson, "Third harmonic generation microscopy," Opt. Express **3**(9), 315–324 (1998).
16. Y. Barad, H. Eisenberg, M. Horowitz, and Y. Silberberg, "Nonlinear scanning laser microscopy by third harmonic generation," Appl. Phys. Lett. **70**(8), 922–924 (1997).
17. P. Kunwar, J. Toivonen, M. Kauranen, and G. Bautista, "Third-harmonic generation imaging of three-dimensional microstructures fabricated by photopolymerization," Opt. Express **24**(9), 9353–9358 (2016).
18. J. Jiao, Y. Gao, S. Li, N. D. Anh, P.-C. Su, S.-W. Kim, C. S. S. Sandeep, and Y.-J. Kim, "Surface third-harmonic generation at a two-photon-polymerized micro-interferometer for real-time on-chip refractive index monitoring," Opt. Express **27**(20), 29196–29206 (2019).
19. L. Turquet, X. Zang, J.-P. Kakko, H. Lipsanen, G. Bautista, and M. Kauranen, "Demonstration of longitudinally polarized optical needles," Opt. Express **26**(21), 27572–27584 (2018).
20. G. Bautista, J.-P. Kakko, V. Dhaka, X. Zang, L. Karvonen, H. Jiang, E. Kauppinen, H. Lipsanen, and M. Kauranen, "Nonlinear microscopy using cylindrical vector beams: Applications to three-dimensional imaging of nanostructures," Opt. Express **25**(11), 12463–12468 (2017).
21. G. Bautista, C. Dreser, X. Zang, D. P. Kern, M. Kauranen, and M. Fleischer, "Collective Effects in Second-Harmonic Generation from Plasmonic Oligomers," Nano Lett. **18**(4), 2571–2580 (2018).
22. H. Lorenz, M. Despont, N. Fahrni, N. LaBianca, P. Renaud, and P. Vettiger, "SU-8: A low-cost negative resist for MEMS," J. Micromech. Microeng. **7**(3), 121–124 (1997).
23. D. C. Meisel, M. Diem, M. Deubel, F. Pérez-Willard, S. Linden, D. Gerthsen, K. Busch, and M. Wegener, "Shrinkage precompensation of holographic three-dimensional photonic-crystal templates," Adv. Mater. **18**(22), 2964–2968 (2006).
24. W. Zhou, S. M. Kuebler, K. L. Braun, T. Yu, J. K. Cammack, C. K. Ober, J. W. Perry, and S. R. Marder, "An efficient two-photon-generated photoacid applied to positive-tone 3D microfabrication," Science **296**(5570), 1106–1109 (2002).